



Metal Nanoparticle Reagents Image in Mouse Bladder With Photothermal Optical Coherence Tomography*

LUO Jia-Xiong**, LI Jian-Cong**, YU Miao, ZENG Ya-Guang, WU Yan-Xiong***

(School of Physics and Optoelectronic Engineering, Foshan University, Foshan 528000, China)

Abstract The paper presents a method to use the photothermal phase difference to map metal nanoparticle (NP) reagent with optical coherence tomography (OCT). The depth-resolved, real-time, and highly localized light-to-heat conversion can be traced by recording the photothermal phase. For adiabatic absorption, the photothermal phase difference represents the localized light absorption characteristics of the NPs. In order to prove the effectiveness of our method, we firstly used FD-OCT imaging system to do agar phantom experiments with different concentrations of NP reagent. The results show that the photothermal phase difference can be used to distinguish different concentrations of NP reagent in agar model. Subsequently, a 3-month-old male C57BL/6J mouse weighing about 25 g was used to verify the feasibility of our method for reconstructing the distribution of NP reagent in tissues. Before the experiment, 0.12 ml chloral hydrate with a concentration of 0.15 g/ml was used for anesthesia, and then 100 μ L NP solution with a concentration of 60 μ g/L was injected into the bladder of mice through a trocar inserted into the urethra. After about 4 hours, the mouse bladder was used to reconstruct the photothermal image. By analyzing the OCT structural image of mouse bladder, we can clearly observe two distinguishable layers. The first layer is detrusor and the second layer is muscularis mucosa. The results are consistent with those reported. In conclusion, we have proved theoretically and experimentally that the distribution of NP reagent in tissues can be reconstructed by photothermal phase difference. Owing to thermal expansion and thermal refractive index effect, the photothermal phase difference can produce local temperature changes in the tissue. For adiabatic absorption, the photothermal phase difference is related to the concentration of NPs. Therefore, it has been used to distinguish different concentrations of NP in the model and reconstruct the distribution of NP in the bladder of mice.

Key words photothermal phase difference, nanoparticle reagents, optical coherence tomography, adiabatic absorption

DOI: 10.16476/j.pibb.2020.0389

Recently, metal nanoparticles (NPs), on account of their unique optical properties, have attracted considerable interest in the biomedical field owing to several applications, such as tumor labels, biological imaging reagents^[1-4]. Complete light energy absorption can be induced in the NPs by illuminating them with an excitation laser at a frequency that matches with their collective plasmon resonance. Because the metal NPs have a very low optical quantum yield, the light energy mainly converts into heat, which simultaneously diffuses to the surrounding. This heat causes thermal expansion and thermal refractive index effect. The phase modulation technique has been demonstrated to map the contrast between the NP reagents in phantoms or biological

tissues. This results in a change in the optical path and introduces a photothermal phase for performing optical coherence tomography (OCT) of the tissues^[5]. Fast Fourier transform algorithm was used to obtain the amplitude of the photothermal vibration excited by a modulation laser^[6-8]. However, the lower

* This work was supported by grants from The National Natural Science Foundation of China (61605026, 61771139, 81601534, 61705036, 61805038) and High-level Construction and Scientific Research Project of Foshan University (CGG07141).

** These authors contributed equally to this work.

*** Corresponding author.

Tel: 86-18943994810, E-mail: winsword@sina.com

Received: October 29, 2020 Accepted: January 20, 2021

modulation frequency is required to obtain a high signal-to-noise ratio and it takes a long acquisition time. Another disadvantage is that the resolved phase amplitude depends not only on the heat generation, which is related to the light absorption, but also on the heat relaxation, which depends on the ambient environment. Therefore, it cannot be used to fully explain the light absorption characteristics of the NP reagents. In this paper, we propose an approach to map the NP reagents using the photothermal phase difference as the image parameter. Compared with the phase modulation, the proposed new method can completely determine the light absorption and accurately map the NP reagents.

1 Materials and methods

When a NP phantom is illuminated by a square wave excitation laser, the heat energy balance equation at the illuminated location is expressed as^[8-9]:

$$\frac{d\Delta T}{dt} = A - B\Delta T, 0 \leq t \leq \tau_0 \quad (1)$$

where ΔT is the temperature change at the illuminated location, A is the rate of energy absorption and proportional to the concentration of the NP, B is the rate constant associated with heat loss, t is time, and τ_0 is the illumination duration of the light. Using the initial condition, $\Delta T(0) = 0$, the general solution of equation (1) is obtained as:

$$\Delta T(t) = \frac{A}{B} (1 - e^{-Bt}), 0 \leq t \leq \tau_0 \quad (2)$$

Equation (2) shows that the temperature change depends on the rate of energy absorption A and rate of heat loss B . For the case of a very short illumination duration, the exponential term can be approximated to: $e^{-Bt} \approx 1 - Bt$, and the increased temperature can be represented as $\Delta T(t) = At$. It means that the temperature increases linearly with the illumination time and the light absorption is an adiabatic process. For a long illumination time, the exponential term becomes zero. The temperature reaches the terminal value $\Delta T(t) = A/B$ and the illuminated location attains thermal equilibrium.

When the excitation laser is turned off, the temperature reaches the maximum value $\Delta T(\tau_0)$ and A disappears in equation (1). Thus, the temperature variation can be acquired from equation (1) as:

$$\Delta T(t) = \Delta T(\tau_0)e^{-Bt}, t > \tau_0 \quad (3)$$

Equation (3) shows that the temperature

exponentially decays after the light is turned off. The heat relaxation depends on B , which is determined by the environment and not the NPs.

Applying the Fourier-domain OCT (FD-OCT) detected light to the laser excited location of the NPs, the depth-resolved interference fringes $B(z,t)$ recorded by a linear charge-coupled device (CCD) can be written as $B(z,t) = r_0(z)\cos(2n_0k_0z + \Delta\varphi(z,t))$, where $\Delta\varphi(z,t)$ denotes the photothermal phase. This $\Delta\varphi(z,t)$ arises from the thermal expansion and thermal refractive index effect and is given by^[7]:

$$\Delta\varphi(z,t) = (2k_0L_0 \frac{dn}{dT} + 2k_0L_0n_0\beta)\Delta T(z,t) \quad (4)$$

where k_0 is the wave vector, β is the volumetric coefficient of expansion, L_0 is the initial physical path length, and n_0 is the refractive index. These parameters can be viewed as constants. Thus, the temperature variation $\Delta T(z,t) = \alpha_0\Delta\varphi(z,t)$ is linearly dependent on the photothermal. If the light absorption is an adiabatic process, the photothermal phase linearly increases with the illuminating time. The depth-resolved $A(z)$ can be obtained from the photothermal phase difference using:

$$A(z) = \alpha_0[\Delta\varphi(z,\tau_0) - \Delta\varphi(z,0)] \quad (5)$$

where $\Delta\varphi(z,\tau_0)$ is the photothermal phase recorded at time τ_0 and $\Delta\varphi(z,0)$ is the initial phase. Since $A(z)$ is related to the depth-resolved NP concentration, it can be used to map the distribution of the NP reagents^[10].

2 Experiment and results

To demonstrate the feasibility of our proposed theory, we used phantom and mouse bladder for *in vitro* imaging of the NP agent. The FD-OCT experimental system is described as follows: a superluminescent diode (SLD) was used as the detected light source with a central wavelength of 1310 nm and bandwidth of 46 nm. It provided an axial resolution of 13 μm in air. In the sample arm, the detected beam and excitation laser with a wavelength of 808 nm and maximum output power of 400 mW were combined using a dichroic mirror *via* an XY pair of scan mirrors. Here, the beams were focused using a 30 mm focal length achromatic objective lens. The diameter of the 808 nm beam was $\sim 50 \mu\text{m}$ at the focused point. A computer was used to synchronously control a linear CCD and generate the square wave to excite the heat laser.

Firstly, we measured the photothermal phase of

the NP phantom using M-scan to verify equation (4). The experimental phantom was a mixture of agar (2%), Au NP particle solution (1% with a concentration of 40 $\mu\text{g/L}$), and water (97%). In our experiment, the acquisition rate of the CCD was set to 8.717 kHz and the total acquired time was 114.7 ms. The excited laser was delayed by 17.72 ms to be triggered relative to the start time of the linear CCD. Figure 1a shows the photothermal phase with an illumination duration of 35.12 ms. The blue line is the trigger signal, black line represents the photothermal phase, and red line shows the fitting profile according to equation (2) (increased phase part) and equation (3) (decay phase part). Figure 1a suggests that the illuminated location attains thermal equilibrium, according to equation (2) (regarding long illumination duration). After the light was turned off, the phase exponentially decays back, as demonstrated by equation (3). Our results are consistent with the experimental results reported in [9]. In this study^[9], a thermocouple was used to trace the temperature change of the NP phantom during the time when the excited light was turned on and off. The dynamic

evolution of the photothermal phase agreed with the temperature variation recorded by the thermocouple. This shows that the photothermal phase is linearly related to the local temperature change as depicted by equation (4). Compared with the previously reported method, our technique can provide a depth-resolved, real-time (microsecond scale), and highly localized (micron scale) light-to-heat conversion trace. Figure 1b shows the photothermal phase signal with an illumination duration of 9.29 ms. The black line shows the raw data and red line is the fitting profile. It clearly shows that the photothermal phase increases linearly with time, as demonstrated in equation (2) (regarding short illumination duration). The slope of the photothermal phase is equal to the rate of energy absorption A . Figure 1b shows that the photothermal phase can record the adiabatic process. Further, by comparing the increased phase part with the decay phase part in figure 1a and 1b, we can find that the heat relaxation duration was longer than the light absorption time. Therefore, the phase modulation amplitude cannot represent the light absorption characteristics of the NP reagents.

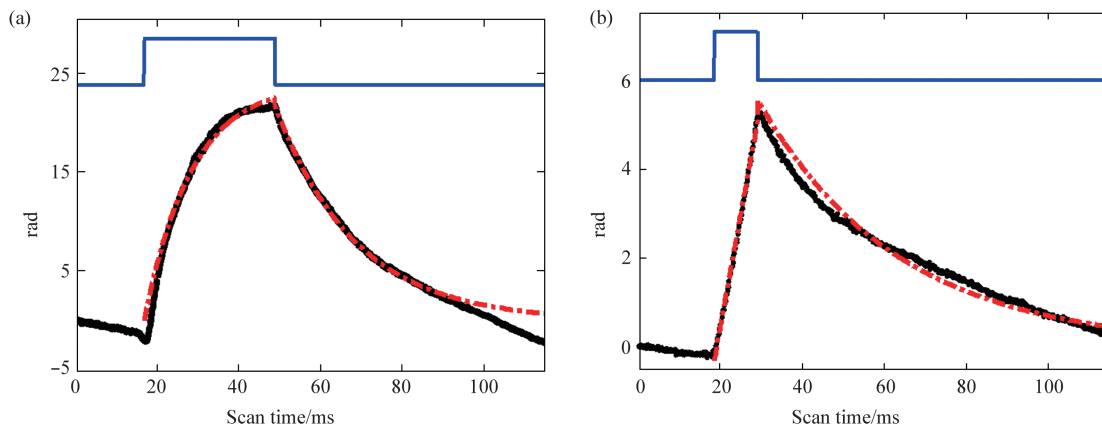


Fig. 1 Photothermal phase signal with an illumination duration of 9.29 ms

(a) Blue profile is the trigger signal, black profile is the photothermal phase excited by the light with duration 35.12 ms, and red profile is the fitting profile based on equation (2) and (3). (b) Black and red profiles are the photothermal phase and their fitting profile excited by the light with duration 9.29 ms, respectively.

Figure 2 shows the different concentrations of the NP phantoms using the photothermal phase difference as the image parameter. Four cylindrical phantoms with the diameter 1.2 mm were made (agar (2%), Au NP particle solution (1% with the different concentrations: no NPs, 20 $\mu\text{g/L}$, 40 $\mu\text{g/L}$, and 60 $\mu\text{g/L}$) and water (97%)). These four phantoms were placed side by side on a glass plane. The output

power of the excitation laser was 30 mW. At every acquired position, only the increased part of the phase was recorded. The total acquired time for the M-scan was 15.94 ms. The excitation laser was delayed by 4.52 ms to be triggered and the illumination duration was $\tau_0=11.42$ ms. The phantoms were covered with a mineral oil to avoid water evaporation during the experiment. Figure 2a shows the OCT structural

image of the NP phantoms, where NP concentrations from left to right are 10 $\mu\text{g/L}$, 20 $\mu\text{g/L}$, 40 $\mu\text{g/L}$, and 60 $\mu\text{g/L}$. No obvious difference in the OCT structural image is observed. It shows that the NPs do not affect the light scattered in the phantoms. Figure 2b shows the photothermal phase difference image of these phantoms. Different concentrations can be differentiated and the intensity of the image increased according to the concentration of the NPs. The photothermal phase $\Delta\varphi(z, \tau_0)$ is the averaged value

recorded from 14.13 ms to 15.94 ms; the initial phase $\Delta\varphi(z, 0)$ is the averaged value during 4.52 ms before the excitation laser was triggered. Because the top of the phantoms were covered by mineral oil, the signal at the top of the phantoms was weaker than that at the bottom. The experimental results indicate that the photothermal phase difference can distinguish among the different concentrations of the NP reagents in the phantoms.

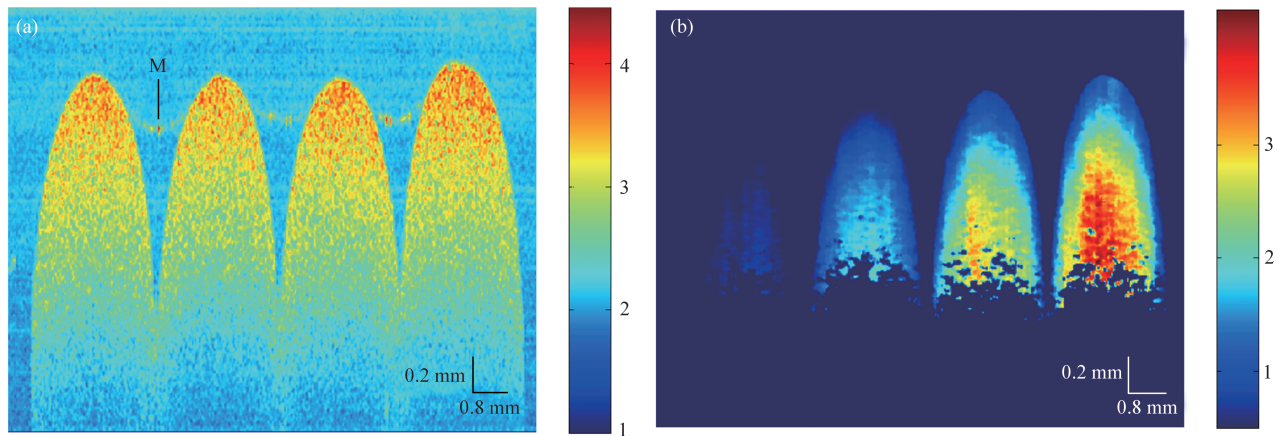


Fig. 2 Comparison of photothermal phase difference images of NP phantoms with different concentrations

(a) OCT structural image of the phantoms with different concentrations (from the left to right: 0 $\mu\text{g/L}$, 20 $\mu\text{g/L}$, 40 $\mu\text{g/L}$, and 60 $\mu\text{g/L}$). M refers to the mineral oil layer. (b) Photothermal phase difference image.

The photothermal phase image of the mouse bladder is shown in Figure 3. We used a three month old male C57BL/6J mouse that weighed 23–28 g. It

was anesthetized with 0.12 ml chloral hydrate at a concentration of 150 g/L. Then, 100 ml NP solution with 60 $\mu\text{g/L}$ concentration of the NPs were injected

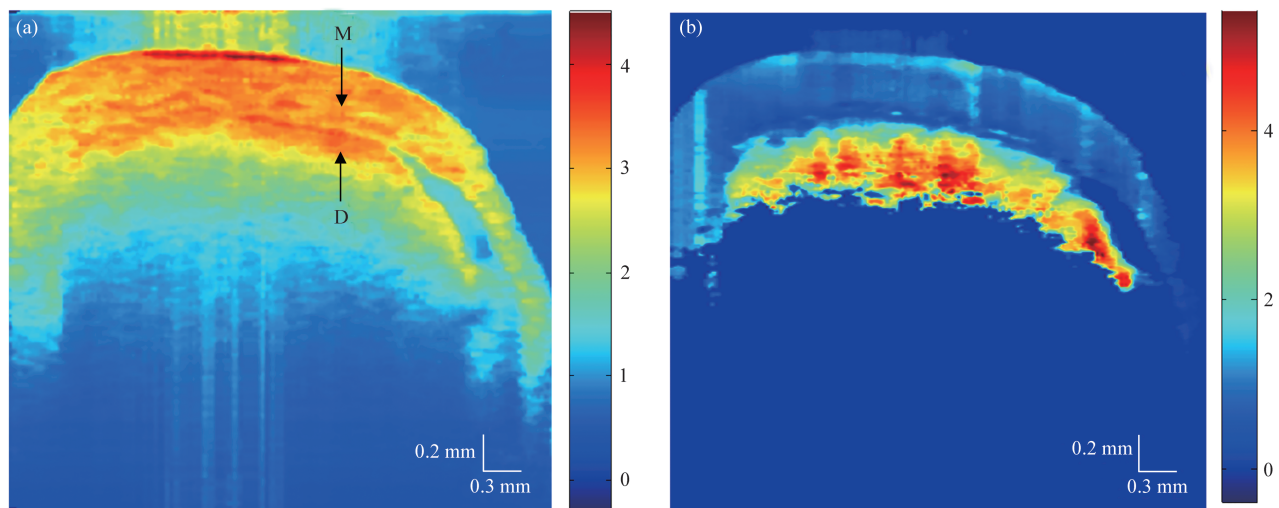


Fig. 3 Photothermal image reconstruction of the mouse bladder

(a) Structural image of the mouse bladder; D presents the detrusor muscle of the bladder; M presents the muscularis mucosa of bladder. (b) Photothermal phase difference image of the mouse bladder.

into the bladder of mice through a trocar inserted into the urethra. After 4 hours, the mouse bladder was used to reconstruct the photothermal image. Figure 3a shows the OCT structural image of the mouse bladder, where we can clearly observe two distinguishable layers. The first layer at the surface is the detrusor muscle of the bladder; the second layer is the muscularis mucosa of the bladder. The results agree with the previous results reported in [11]. Figure 3b shows the photothermal phase difference image of the bladder. Compared with the OCT structural image, the signal of the detrusor muscle layer is stronger than that of the muscularis mucosa layer. It shows that the NP was deposited on the detrusor muscle layer. This result is logical because the muscularis mucosa layer is close to the urinary tract inside the bladder. Thus, we can infer that the photothermal phase difference could be used to map the NP agent distribution in a tissue.

3 Discussion and conclusion

In conclusion, we theoretically and experimentally demonstrate the reconstruction of the NP agent distribution in a tissue using the photothermal phase difference. Owing to the thermal expansion and thermal refractive index effect, the photothermal phase can yield the local temperature variation in a tissue. For adiabatic absorption, the photothermal phase difference is related to the concentration of NPs, and was thus, used to image the concentration of NPs in the phantoms and NP agent distribution in the mouse bladder. In addition, the imaging is limited by the thickness of the sample. In this paper, the reconstruction of NP agent distribution in the mouse bladder can meet the requirements of thickness for imaging system.

References

- [1] Lee T M, Oldenburg A L, Sitafulwalla S, *et al.* Engineered microsphere contrast agents for optical coherence tomography. *Optics Letters*, 2003, **28**(17): 1546-1548
- [2] Yu P, Mustata M, Peng L, *et al.* Holographic optical coherence imaging of rat osteogenic sarcoma tumor spheroids. *Applied Optics*, 2004, **43**(25): 4862-4873
- [3] Tamarat P, Choquet D, Cognet L, *et al.* Single metallic nanoparticle imaging for protein detection in cells. *Proc Natl Acad Sci USA*, 2003, **100**(20): 11350-11355
- [4] Gobin A M, Lee M H, Halas N J, *et al.* Near-infrared resonant nanoshells for combined optical imaging and photothermal cancer therapy. *Nano Letters*, 2007, **7**(7): 1929-1934
- [5] Telenkov S A, Dave D P, Sethuraman S, *et al.* Differential phase optical coherence probe for depth-resolved detection of photothermal response in tissue. *Physics in Medicine & Biology*, 2004, **49**(1): 111-119
- [6] Skala Melissa C, Crow Matthew J, Wax A, *et al.* Photothermal optical coherence tomography of epidermal growth factor receptor in live cells using immunotargeted gold nanospheres. *Nano Letters*, 2008, **8**(10): 3461-3467
- [7] Adler D C, Huang S W, Huber R, *et al.* Photothermal detection of gold nanoparticles using phase-sensitive optical coherence tomography. *Opt Express*, 2008, **16**(3): 4376-4393
- [8] Zhou C, Tsai T H, Adler D C, *et al.* Photothermal optical coherence tomography in *ex vivo* human breast tissues using gold nanoshells. *Optics Letters*, 2010, **35**(5): 700-702
- [9] Richardson H H, Carlson M T, Tandler P J, *et al.* Experimental and theoretical studies of light-to-heat conversion and collective heating effects in metal nanoparticle solutions. *Nano Letters*, 2009, **9**(3): 1139-1146
- [10] Hoepfner M, Roper D K, Ahn W. Microscale heat transfer transduced by surface plasmon resonant gold nanoparticles. *J Phys Chem C Nanomater Interfaces*, 2007, **111**(9): 3636-3641
- [11] Xie T Q, Zeidel M L, Pan Y. Detection of tumorigenesis in urinary bladder with optical coherence tomography: optical characterization of morphological changes. *Optics Express*, 2002, **10**(24): 1431-1443

小鼠膀胱内金属纳米粒子的光热 光学相干层析成像*

罗佳雄** 李建聪** 余 苗 曾亚光 伍雁雄***

(佛山科学技术学院物理与光电工程学院, 佛山 528000)

摘要 本文提出了一种利用光热相差对金属纳米粒子 (NP) 试剂进行光学相干层析成像 (OCT) 的方法. 通过记录光热相位, 可以跟踪深度可分辨、实时和高度局部化的光热转换. 对于绝热吸收, 光热相差代表了 NP 的局部光吸收特性. 为了验证该方法的有效性, 我们首先利用 FD-OCT 成像系统对不同浓度的 NP 试剂进行了琼脂体模实验. 结果表明, 光热相位差可以用来区分琼脂体模中不同浓度的 NP 试剂. 随后, 一只体重约为 25 g 的 3 月龄雄性 C57BL/6J 小鼠被用来验证在组织中重建 NP 试剂分布方法的可行性. 实验前先用 0.12 ml 浓度为 0.15 g/ml 的水合氯醛麻醉, 然后通过插入尿道的套管针将 100 μ l 浓度为 60 μ g/L 的 NP 试剂注入小鼠膀胱内. 大约 4 h 后, 用小鼠膀胱重建光热图像. 通过分析小鼠膀胱的 OCT 结构图像, 可以清晰地观察到两个可分辨的层. 第一层为逼尿肌, 第二层为黏膜肌层. 总之, 我们从理论和实验证明了利用光热相差可以重建 NP 试剂在组织中的分布. 由于热膨胀和热折射率效应, 光热相差会引起组织局部温度的变化. 对于绝热吸收, 光热相差与 NP 试剂的浓度有关. 因此, 该方法可用于区分模型中不同浓度的 NP 试剂, 并重建 NP 试剂在小鼠膀胱中的分布.

关键词 光热相差, 纳米粒子剂, 光学相干层析成像, 绝热吸收

中图分类号 O445

DOI: 10.16476/j.pibb.2020.0389

* 国家自然科学基金 (61605026, 61771139, 81601534, 61705036, 61805038) 和佛山科学技术学院高层次建设与科研项目 (CGG07141) 资助.

** 并列第一作者.

*** 通讯联系人.

Tel: 18943994810, E-mail: winsword@sina.com

收稿日期: 2020-10-29, 接受日期: 2021-01-20